Environmental Pollution 344 (2024) 123316

Contents lists available at ScienceDirect

Environmental Pollution

journal homepage: www.elsevier.com/locate/envpol

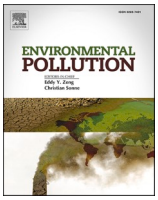

Investigating strontium isotope linkage between biominerals (uroliths), drinking water and environmental matrices☆

F. Izzo [a], V. Di Renzo [a], A. Langella [a,*], M. D'Antonio [a], P. Tranfa [a], D. Widory [b], L. Salzano [c], C. Germinario [d], C. Grifa [d], E. Varricchio [d], M. Mercurio [d]

[a] Department of Earth Sciences, Environment and Resources, University of Naples Federico II, via Cintia, Naples, 80126, Italy
[b] Geotop/Université du Québec a Montréal (UQAM), 201 Ave Président Kennedy, Montréal, QC, H2X 3Y7, Canada
[c] UOC Urology, San Pio Hospital, Via dell'Angelo, 82100, Benevento, Italy
[d] Department of Science and Technology, University of Sannio, via de Sanctis snc, Benevento, 82100, Italy

ARTICLE INFO

Keywords:
Biomineralogy
Strontium isotope geochemistry
Environment
Health
Waters
Exposure

ABSTRACT

This study presents the mineralogy and strontium isotope ratio ($^{87}Sr/^{86}Sr$) of 21 pathological biominerals (bladder and kidney stones) collected from patients admitted between 2018 and 2020 at the Department of Urology of the San Pio Hospital (Benevento, southern Italy). Urinary stones belong to the calcium oxalate, purine or calcium phosphate mineralogy types. Their corresponding $^{87}Sr/^{86}Sr$ range from 0.707607 for an uricite sample to 0.709970 for a weddellite one, and seem to be partly discriminated based on the mineralogy. The comparison with the isotope characteristics of 38 representative Italian bottled and tap drinking waters show a general overlap in $^{87}Sr/^{86}Sr$ with the biominerals. However, on a smaller geographic area (Campania Region), we observe small $^{87}Sr/^{86}Sr$ differences between the biominerals and local waters. This may be explained by external Sr inputs for example from agriculture practices, inhaled aerosols (i.e., particulate matter), animal manure and sewage, non-regional foods. Nevertheless, biominerals of patients that stated to drink and eat local water/wines and foods every day exhibited a narrower $^{87}Sr/^{86}Sr$ range roughly matching the typical isotope ratios of local geological materials and waters, as well as those of archaeological biominerals from the same area.

Finally, we conclude that the strontium isotope signature of urinary stones may reflect that of the environmental matrices surrounding patients, but future investigations are recommended to ultimately establish the potential for pathological biominerals as reliable biomonitoring proxies, taking into the account the contribution of the external sources of Sr.

1. Introduction

Urolithiasis is a pathological and multifactorial biomineralization process that mainly concerns adult populations worldwide, and for which a constant rising incidence has been observed in developed countries (Sorokin et al., 2017). Uroliths are symptomatic of various diseases and exhibit numerous qualitative and quantitative mineralogical compositions. Morpho-constitutional classification schemes (Cloutier et al., 2015; Daudon et al., 2016) identify seven distinct types of calculi: type I, whewellite (calcium oxalate monohydrate, COM); type II, weddellite (calcium oxalate dihydrate, COD); type III, uric acid and urate; type IV, phosphate stones; type V, cystine; type VI, protein; type VII, miscellaneous stones. Among them, calcium stones, such as oxalates and phosphates, along with uric acids, represent the most frequent biomineralogical products of human urolithiasis. To date, althought valuable to set preventive measures and plan proper therapeutical approaches, the conventional classification of these biominerals has not proven to be able to reveal the interactions that may exist between the charateristics of the patient's uroliths and his everyday life environment. In contrast, more complex and in-depth analytical approaches, have started providing insights into these potential links. A particular attention has been put to characterize both their major (>1 wt%) and trace elements (<1 wt%) chemical composition, and to correlate them with metabolic processes, daily food, drink intakes and environmental factors (Bazin et al., 2007; Diangienda et al., 2021; Giannossi et al., 2013; Singh and Rai, 2014). Some investigations have shown that trace elements

☆ This paper has been recommended for acceptance by Hefa Cheng.

* Corresponding author.
E-mail address: alessio.langella@unina.it (A. Langella).

https://doi.org/10.1016/j.envpol.2024.123316
Received 11 September 2023; Received in revised form 12 December 2023; Accepted 4 January 2024
Available online 5 January 2024

generally act as promoters or inhibitors of the urolithiasis process (Basavaraj et al., 2007; Frassetto and Kohlstadt, 2011). Patient's exposure to a polluted environment or the ingestion of contaminated food/drink can lead to the incorporation of undesired elements such as Cu, Cd, Pb, Cr, Hg and As in the crystal lattices of the biominerals that will ultimately form the urinary stones (Kuta et al., 2013, 2012; Pal'chik et al., 2006), and are thus considered common environmental nephrotoxic metal pollutants (Huang et al., 2023; Jain, 2020; Sun et al., 2019; Thomas et al., 2013). These noxious substances have been recently observed in some bladder stones from patients admitted to the San Pio Hospital in Benevento (South Italy), as reported in Mercurio et al., 2022. The authors emphasized the tendency for oxalates and phosphates to drive the ionic substitution of both desired and undesired elements, even when these Ca-bearing biominerals occur as traces or minor components in the organic crystals (i.e., uric acids) (Mercurio et al., 2022). Moreover, a potential correlation exists between pathological biomineralizations and the environmental/geological settings surrounding the patient that could be inferred by an accurate analysis of trace elements forming the biominerals and their isotopic compositions (Abdel-Gawad et al., 2022; Athanasiadou, 2017; Athanasiadou et al., 2013; Chandrajith et al., 2019; Wang et al., 2019).

Due to its peculiar geochemical features, strontium (Sr) is ubiquitous in the environment, present in several reservoirs such as soils, plants and water. Geological provinces are usually characterized by specific narrow ranges of strontium isotope ratios ($^{87}Sr/^{86}Sr$). $^{87}Sr/^{86}Sr$ is inherited from the local geological substrate as a result of a combination of initial rubidium (Rb) content and age: ^{87}Rb decays into ^{87}Sr over time, and subsequently causes a slow increase of the $^{87}Sr/^{86}Sr$ isotope ratio with time (Faure and Mensing, 2004). The chemical weathering of sedimentary, metamorphic and magmatic rocks at the Earth surface, as well as water-rock interaction release Sr^{2+} ions that penetrate the ecosystem and accumulate in waters and soils. In soils, Sr is mainly present in the inorganic fraction (mineral and rock fragments) whereas the bioavailable fraction represents the part that can be exchanged with water and plants. Bioavailable Sr eventually enters the human body with no isotope fractionation, thus preserving its initial $^{87}Sr/^{86}Sr$ ratio. It follows that $^{87}Sr/^{86}Sr$ ratios have been used as tracers in human tissues as they reflect the isotope characteristics of the environment in which people have lived (Capo et al., 1998; Stewart et al., 1998). Bones and teeth, which similarly to uroliths are considered as the end-products of biomineralization processes, preserve intact the initial $^{87}Sr/^{86}Sr$ ratios of the environment from which Sr originates (see for example Coelho et al., 2017). To date, this assumption has not yet been proved for uroliths (pathological biominerals), as the metabolism and physiology of stone formers (referred to as "vital effects") may modify their final Sr isotope ratios. Morover, the capacity for biominerals to incorporate Sr^{2+} ions into their lattice depends on both their crystal structure and crystal chemistry.

With that in mind, our objective here was to use $^{87}Sr/^{86}Sr$ ratio, a peculiar geochemical tracer routinely used for interpreting geological processes (Faure and Mensing, 2004), to correlate the characteristics of patients' urolith and their lifestyle habits, trying to identify correlations with direct or indirect contacts with their geological and environmental surroundings (water, soil, rock, etc.). Analyzed samples consisted of 21 kidney and bladder stones that were collected at the Department of Urology of the San Pio Hospital (Benevento, Italy) from patients living in Campania Region admitted between 2018 and 2020, and for which both a mineralogical and morphological characterization had already been undertaken (details in Izzo et al., 2022; Mercurio et al., 2022).

Investigation was also extended to a vital fluid for humans such as water. Local tap waters and bottle waters from totally different Italian areas were here analyzed in order to highlight if and how different geological and hydrogeological settings could influence their Sr isotope ratio characterizing the connections existing between humans and their surrounding environment. Therefore, our investigation mainly aims to a more comprehensive interpretation of isotope ratios in human uroliths, by integrating the uroliths mineralogical composition and type and evaluating how dietary habits may affect such fingerprint.

1.1. Strontium: brief overview inside the matter of the biominerals

Strontium (Sr), one of the most common lithophile metals, is a highly reactive alkaline earth metal present in the nature as Sr^{2+}. In urinary stones, it is a trace element, with concentrations typically ranging from a few to ~500 ppm (e.g., Tian et al., 2022). Sr has an atomic radius and an electron configuration that are similar to those of calcium (Ca). It can thus substitute to Ca^{2+} in the mineral lattice of various rocks and other solid environmental matrices, explaining why it is also found in uroliths. For humans the primary Sr exposure sources are drinking water (an adult drinking 2 L of water per day could ingests up to 2.2 mg of Sr) and food (grains, leafy vegetables and dairy products) (WHO, 2010). On average, the world population ingests 1.2–2.4 mg Sr/person/day, mainly through the consumption of eggs, vegetables and fruits, cereal products, fish, and meat. Respiration is generally considered a minor contributor to Sr intake, except for people living next to Sr emission sources. Sr is absorbed through the gastrointestinal tract and is primarily excreted in urine and faeces. The distribution of absorbed Sr in the human body is similar to that of calcium, with approximately 99% of the total body burden being in the skeleton.

The study of Sr isotope ratios ($^{87}Sr/^{86}Sr$) has already demonstrated its added value for fingerprinting biominerals and environmental matrices, especially in biology-related fields (Coelho et al., 2017; Holt et al., 2021) such as forensic sciences, medical application, bioarchaeology, archaeometry, and food provenance (see D'Antonio et al., 2023 for a review). In bones and teeth, Sr can replace calcium without modifying the $^{87}Sr/^{86}Sr$ ratios between its source (e.g., food and local environmental matrices) and target (e.g., tissue) (Crowley et al., 2017). Thus, $^{87}Sr/^{86}Sr$ ratios in human tissues have been widely used to track human mobility (Arienzo et al., 2020; Font et al., 2012; Frei and Price, 2012; Kenoyer et al., 2013; Price et al., 2008; Price and Gestsdóttir, 2006; Stantis et al., 2015). This is usually based on the possibility to compare $^{87}Sr/^{86}Sr$ ratios of human tissues with published Sr isoscapes (i.e., mapping of geological isotope ratio distribution) (Bataille et al., 2018; Holt et al., 2021; James et al., 2022; Lugli et al., 2022; Wang and Tang, 2020).

To our knowledge, the only research carried out on strontium isotope ratios in human kidney stones was recently published by Qu et al. (2023). The authors reported the first $^{87}Sr/^{86}Sr$ ratios in 17 samples of calcium oxalate kidney stones collected from patients in Beijing (China), showing an isotope correlation between the bioavailable Sr of these urinary stones and local drinking waters and food.

2. Materials

2.1. Biominerals

The 21 biominerals were surgically collected from as many patients who had been admitted at the San Pio Hospital of Benevento (South Italy). Samples consisted of both bladder (n = 16) and kidney stones (n = 5). Samples were labelled using the abbreviation code KS (namely kidney stones) followed by a sequential number (Table 1). Where appropriate, the letter B was added to specifically identify the bladder stone samples. All patients were subjected to anonymized clinical interviews to document their medical history and lifestyle (Izzo et al., 2022; Mercurio et al., 2022). Biominerals have been previously classified based on their mineralogy and morphology, and showed that they were corresponding to 7 calcium oxalates [$CaC_2O_4{\cdot}nH_2O$], 12 purines (11 uric acids [$C_5H_4N_4O_3$] and 1 ammonium urate [$NH_4C_5H_3N_4O_3$]), and 2 calcium phosphates (1 carbonate apatite [$Ca_5(PO_4,CO_3)_3(OH,F)$] and 1 brushite [$CaHPO_4{\cdot}2H_2O$]) (Table 1). All samples corresponded to patients who lived in the Campania region (Fig. 1).

Table 1
Morpho-constitutional classification of the examined urinary stones (Izzo et al., 2022; Mercurio et al., 2022) and their corresponding strontium isotope ratios ($^{87}Sr/^{86}Sr$). Place of residence has been also reported (provinces in brackets).

n.	ID	Municipality	Type	Main composition	$^{87}Sr/^{86}Sr$	2 s.e.
1	KS012B	Torrecuso (BN)	Ia	CaOx; CaP (tr.)	0.708735*	±0.000004
2	KS030	San Giorgio del Sannio (BN)	Ia	CaOx; CaP (tr.)	0.709077*	±0.000006
3	KS047	Castelvetere (BN)	Ia/IIb/IVa	CaOx; CaP	0.708613	±0.000005
4	KS033B	Amorosi (BN)	Ie	CaOx; CaP (tr.)	0.708572*	±0.000007
5	KS028B	Frasso Telesino (BN)	IIb	CaOx; CaP (tr.)	0.709167*	±0.000005
6	KS036B	Sant'Egidio del Monte Albino (SA)	IIb	CaOx; CaP (tr.), O.M. (tr.)	0.709970	±0.000007
7	KS040	Montefalcone di Val Fortore (BN)	IIb	CaOx; CaP (tr.)	0.708716	±0.000007
8	KS046	Colle Sannita (BN)	III	UA	0.709499*	±0.000012
9	KS011B	Andretta (AV)	IIIa	UA; CaOx (tr.)	0.708506*	±0.000013
10	KS023B	Durazzano (CE)	IIIa	UA	0.708321	±0.000007
11	KS029B	Ponte (BN)	IIIa	UA	0.708712*	±0.000010
12	KS034B	San Giorgio del Sannio (BN)	IIIa	UA	0.708499	±0.000008
13	KS035B	Torrecuso (BN)	IIIa	UA	0.708438	±0.000006
14	KS037B	Cervinara (AV)	IIIa	UA; CaOx (tr.)	0.708246	±0.000007
15	KS050B	Baselice (BN)	IIIa	UA; O.M. (tr.)	0.708726	±0.000011
16	KS022B	Aquilonia (AV)	IIIa/IIIb	UA; CaOx (tr.)	0.709263	±0.000011
17	KS020B	Lacedonia (AV)	IIIb	UA	0.707607	±0.000010
18	KS043	Boscotrecase (NA)	IIIb	UA; CaOx (tr.)	0.708738	±0.000007
19	KS041	San Lorenzo Maggiore (BN)	IIIc/Ia/IIb	AU/CaOx; CaP (tr.)	0.708747	±0.000008
20	KS032B	Procida (NA)	IVa/IIa	CaP/CaOx	0.708618*	±0.000006
21	KS006B	San Leucio del Sannio (BN)	IVd	Br; CaOx (tr.), CaP (tr.)	0.708736	±0.000008

2 s.e. = 2 x standard error on 150 cycles (isotope ratio acquisitions). $^{87}Sr/^{86}Sr$ ratios are already normalized to the mean value of the NIST-SRM 987 international standard. Note: AV, Avellino; BN, Benevento; CE, Caserta; NA, Napoli; SA, Salerno; CaOx, calcium oxalate; CaP, calcium phosphate; UA, uric acid; AU, ammonium urate; Br, brushite; O.M., organic matter; (tr.), trace; *, weighted average obtained from replicate measurements.

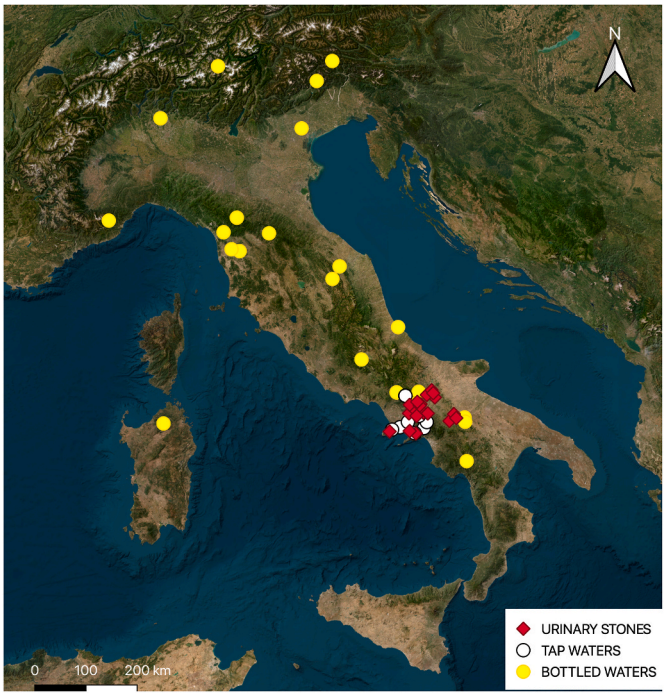

Fig. 1. Biomineral and drinking water samples locations.

2.2. Drinking waters

38 drinking water samples were also collected and analyzed for their Sr-isotope ratios, for comparison purposes: 28 bottled waters and 10 tap waters. Bottled waters (BW) were produced from various springs located in Italy (Fig. 1) and corresponded to distinct geological settings (Table 2). Based on the Total Dissolved Solids (TDS) criterion (van der Aa, 2003) and according to TDS values reported on bottle labels, only sample BW5 corresponded to a high mineral concentration (TDS >1500 mg/L), whereas samples BW4, BW8, BW9, BW24 and BW25 showed intermediate mineral concentrations (TDS 500–1500 mg/L). The remaining samples were classified as low mineralized (TDS <500 mg/L). All tap water samples (TW) were collected in the Campania region (Fig. 1), in the provinces of Caserta (TW1 and TW2), Naples (TW3-TW5), Benevento (TW6), Avellino (TW7-TW9), and Salerno (TW10) (Table 2). All tap waters derive from sedimentary aquifers and are municipally feed. Samples were collected in fresh sterile plastic containers. Unfortunately, TDS information was not available for the examined samples. Still, Italian tap waters are generally intermediate or, subordinately, low mineralized (Ministry of Health, 2016).

3. Methods

Sample preparation, as well as geochemical and isotope analyses were carried out at the Department of Earth Sciences, Environment and Resources, University of Napoli Federico II (Italy). Urinary stones and drinking waters were prepared for Sr-isotope ratio determination in an ISO 6 – ISO 5 clean room. The step-by-step procedure for Sr separation is described in Fig. 2 for each type of sample (tap water, bottled water and urinary stones). Chemical dissolution was carried out using Suprapur® reagents, diluted with Milli-Q® deionized water when necessary. About 0.05 g of each KS sample were dissolved adding 0.25 mL HNO_3 (65%) +1.5 mL HF (40%) in a PTFE vial placed overnight on a hot plate at 110 °C under a laminar flow hood. The sample was then ultrasonicated 8 min and evaporated to dryness at 110 °C. Remaining organic matter was removed from the urolith samples with 3 cycles of alternating 0.1 mL HNO_3 (65%) and H_2O_2 (30%). 0.75 mL of HNO_3 (65%) were then added and the sample was once again evaporated to dryness on hot plate at 110 °C. 2 mL HCl 6N were then added and the samples placed overnight on a hot plate at 110 °C under a laminar flow hood. Finally, samples were taken up in 1 mL HCl 2.5N and centrifuged at 4500 rpm for 10 min. Strontium was chromatographically separated from the liquid matrix using quartz columns filled with 2 mL of cation exchange resin Dowex AG 50 W X-8 (200–400 mesh), following the protocol described in Arienzo et al. (2013).

The analytical procedure for Sr separation of drinking waters is also presented in Fig. 2. About 15 mL of each sample were put into PTFE vials on a hot plate at 80 °C under a laminar flow hood for 24h. When dried, samples were taken up in 1 mL HCl 2.5N and centrifuged at 4500 rpm for 10 min. The water aliquot required for chemical processing was taken up

Table 2
Characteristics of Italian bottled and tap waters and their strontium isotope ratios.

n.	ID	Municipality	Region	Type	TDS (mg/L)	Main lithology of the aquifer	$^{87}Sr/^{86}Sr$	2 s.e.
1	BW1	Montesano sulla Marcellana (SA)	Campania	Still	245	Mesozoic carbonate-rocks	0.707827	±0.000007
2	BW2	Pratella (CE)	Campania	Still	270	Mesozoic carbonate-rocks	0.708062	±0.000006
3	BW3	Pratella (CE)	Campania	Sparkling	270	Mesozoic carbonate-rocks	0.708065	±0.000007
4	BW4	Pratella (CE)	Campania	Sparkling	845	Mesozoic carbonate-rocks	0.707835*	±0.000004
5	BW5	Telese (BN)	Campania	Sparkling	1858	Mesozoic carbonate-rocks	0.707635*	±0.000007
6	BW6	Canistro Inferiore (AQ)	Abruzzo	Still	260	Mesozoic carbonate-rocks	0.708468	±0.000006
7	BW7	Pescara (PE)	Abruzzo	Still	289	Late Pliocene - Holocene alluvial and hemipelagic calcareous sedimentary rocks	0.707982	±0.000006
8	BW8	Melfi (PZ)	Basilicata	Sparkling	1183	Quaternary volcanic rocks	0.706056*	±0.000005
9	BW9	Rionero in Vulture (PZ)	Basilicata	Sparkling	1200	Quaternary volcanic rocks	0.706055	±0.000006
10	BW10	Viggianello (PZ)	Basilicata	Still	154	Mesozoic carbonate-rocks	0.707967	±0.000006
11	BW11	Monte Cimone (MO)	Emilia-Romagna	Sparkling	128	Cenozoic sedimentary siliciclastic rocks	0.709192	±0.000007
12	BW12	Monte Cimone (MO)	Emilia-Romagna	Still	128	Cenozoic sedimentary siliciclastic rocks	0.709213	±0.000006
12	BW13	Forni Avoltri (UD)	Friuli-Venezia Giulia	Still	74	Palaeozoic metamorphic rocks	0.717474	±0.000006
14	BW14	Cimolais (PN)	Friuli-Venezia Giulia	Still	118	Mesozoic carbonate-rocks	0.707950	±0.000006
15	BW15	Cadorago (CO)	Lombardy	Still	132	Quaternary glacial deposits	0.709413	±0.000007
16	BW16	Cadorago (CO)	Lombardy	Sparkling	132	Quaternary glacial deposits	0.709407	±0.000006
17	BW17	Valdidentro (SO)	Lombardy	Still	80	Palaeozoic metamorphic rocks	0.727360*	±0.000006
18	BW18	Gola della Rossa e di Frasassi (AN)	Marche	Still	339	Mesozoic carbonate-rocks	0.707673	±0.000007
19	BW19	Gola della Rossa e di Frasassi (AN)	Marche	Sparkling	339	Mesozoic carbonate-rocks	0.707671	±0.000007
20	BW20	Sepino (CB)	Molise	Still	277	Mesozoic carbonate-rocks	0.707809	±0.000006
21	BW21	Tempio Pausania (SS)	Sardinia	Still	157	Palaeozoic intrusive rocks	0.709712	±0.000007
22	BW22	Pescaglia (LU)	Tuscany	Still	242	Late-Pliocene calcareous hemipelagic sedimentary rocks	0.708886	±0.000007
23	BW23	Pescaglia (LU)	Tuscany	Sparkling	242	Late-Pliocene calcareous hemipelagic sedimentary rocks	0.708868	±0.000007
24	BW24	Montopoli in Val d'Arno (PI)	Tuscany	Still	575	Cenozoic sedimentary siliciclastic rocks	0.709069	±0.000006
25	BW25	Vicopisano (PI)	Tuscany	Still	741	Mesozoic carbonate-rocks	0.708453*	±0.000007
26	BW26	Scarperia e San Piero (FI)	Tuscany	Still	139	Cenozoic calcareous and siliciclastic sedimentary rocks	0.709587*	±0.000004
27	BW27	Gualdo Tadino (PG)	Umbria	Still	182	Mesozoic carbonate-rocks	0.707752	±0.000006
28	BW28	Ormea	Piedmont	Still	113	Palaeozoic intrusive rocks	0.712359*	±0.000004
29	TW1	Piedimonte Matese (CE)	Campania	Still	–	Mesozoic carbonate-rocks	0.707822	±0.000006
30	TW2	Piedimonte Matese (CE)	Campania	Still	–	Mesozoic carbonate-rocks	0.707799	±0.000006
31	TW3	Naples (NA)	Campania	Still	–	Mesozoic carbonate-rocks	0.707748*	±0.000004
32	TW4	Brusciano (NA)	Campania	Still	–	Mesozoic carbonate-rocks	0.707740*	±0.000004
33	TW5	Bacoli (NA)	Campania	Still	–	Mesozoic carbonate-rocks	0.707869	±0.000006
34	TW6	Ceppaloni (BN)	Campania	Still	–	Mesozoic carbonate-rocks	0.707749	±0.000006
35	TW7	Montoro (AV)	Campania	Still	–	Mesozoic carbonate-rocks	0.707748	±0.000006
36	TW8	Atripalda (AV)	Campania	Still	–	Mesozoic carbonate-rocks	0.707659*	±0.000005
37	TW9	San Martino Valle Caudina (AV)	Campania	Still	–	Mesozoic carbonate-rocks	0.707840	±0.000006
38	TW10	Angri (SA)	Campania	Still	–	Mesozoic carbonate-rocks	0.707693*	±0.000005

2 s.e. = 2 x standard error on 150 cycles (isotope ratio acquisitions). $^{87}Sr/^{86}Sr$ ratios are already normalized to the mean value of the NIST-SRM 987 international standard. TDS, Total Dissolved Solids; SA, Salerno; CB, Campobasso; CE, Caserta; BN, Benevento; AQ, L'Aquila; PE, Pescara; PZ, Potenza; MO, Modena; UD, Udine; PN, Pordenone; FR, Frosinone; CO, Como; SO, Sondrio; AN, Ancona; SS, Sassari; LU, Lucca; PI, Pisa; PG, Perugia.
*, weighted average obtained from replicate measurements.

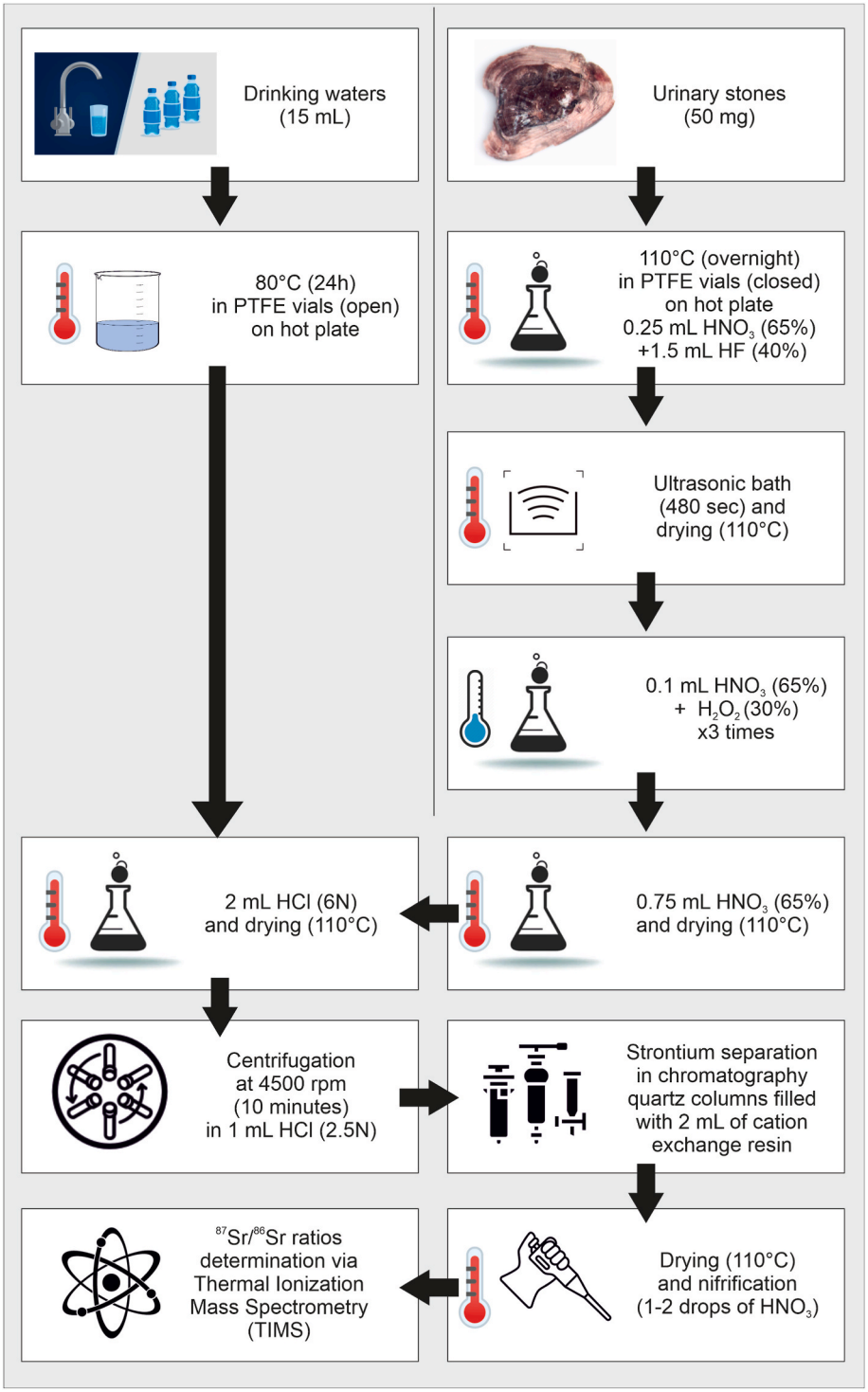

Fig. 2. Analytical procedure for the preparation and purification of strontium for $^{87}Sr/^{86}Sr$ analysis in tap water, bottled water and urinary stone samples.

directly from the sterile containers for tap waters and from purchased bottles for bottled still waters. The Sr purification step was achieved following the same procedure as for urinary stones.

Ultimately, elution solutions, containing pure Sr from either urinary stone or water, were put to dryness at 110 °C on a hot plate under laminar flow hood and nitrified by adding 1–2 drops of concentrated HNO_3. The corresponding $^{87}Sr/^{86}Sr$ ratios were then determined on a ThermoScientific Triton Plus® Thermal Ionization Mass Spectrometer (TIMS). During the period of data collection, the external 2σ reproducibility (σ = standard deviation) as proposed by Goldstein et al. (2003) was checked by the replicate analysis of the NIST–SRM 987 international standard, that provided a mean $^{87}Sr/^{86}Sr$ of 0.710243 ± 0.000010 (2σ, n = 29). Accordingly, sample $^{87}Sr/^{86}Sr$ ratios were normalized to the value recommended for NIST–SRM 987 (i.e., $^{87}Sr/^{86}Sr$ = 0.710248; Zhang and Hu, 2020). Each analysis comprised 150 single acquisitions (cycles) of several Sr-isotope ratios involving the four Sr isotopes. The final $^{87}Sr/^{86}Sr$ was corrected for in-run isotope fractionation by normalizing the $^{88}Sr/^{86}Sr$ ratio to its natural value of 8.37521, through an exponential law. The total procedure Sr blank is on average 100 pg. List of replicate measurements is reported in supplementary material

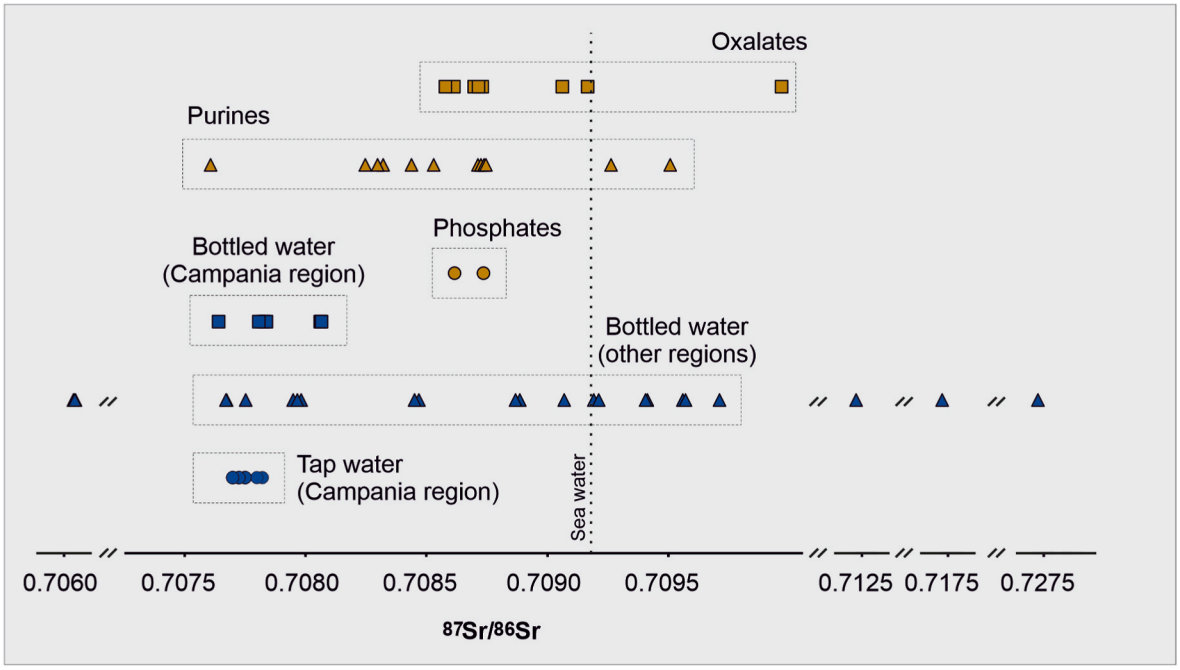

Fig. 3. Ranges of strontium isotope ratios measured in urinary stones and drinking waters. The seawater Sr isotope-ratio ($^{87}Sr/^{86}Sr = 0.70919$), measured in the gulf of Naples, is taken from Arienzo et al. (2016).

(Table S2). Strontium and Calcium in urinary stones were measured by ICP-OES (Avio 200 PerkinElmer) whereas the same elements were taken from literature for drinking waters (Cicchella et al., 2010; Dinelli et al., 2012).

4. Results

Investigated urinary stones, as a whole, display a rather large range of $^{87}Sr/^{86}Sr$ ratios (Table 1 and Fig. 3), from 0.707607 for the bladder stone KS020B, mainly formed by uricite (Type IIIb, ideal composition [$C_5H_4N_4O_3$]), to 0.709970 for the bladder stone KS036B, made of weddellite (Type IIb, ideal composition [$CaC_2O_4{\cdot}(2+x)H_2O$], where $x < 1$), with an average $^{87}Sr/^{86}Sr$ of 0.70873 ± 0.00048 (1σ; n = 21). Purines yield the largest isotope variability, with $^{87}Sr/^{86}Sr$ between 0.707607 (sample KS020B) and 0.709263 (sample KS022B), with an average $^{87}Sr/^{86}Sr$ of 0.70851 ± 0.00049 (1σ; n = 12). Oxalate samples show a slightly higher average isotope ratio ($^{87}Sr/^{86}Sr = 0.70894 \pm 0.00047$; 1σ; n = 7), with sample KS036B having the highest value of all ($^{87}Sr/^{86}Sr = 0.709970$). Among purines, the kidney stone (KS041), a mixture of oxalates (including whewellite [$CaC_2O_4{\cdot}H_2O$]) and ammonium urate (ideal composition [$NH_4C_5H_3N_4O_3$]), exhibits an intermediate $^{87}Sr/^{86}Sr$ ratio of 0.70875 (Table 1). Phosphate-based uroliths show the narrowest isotope range (average $^{87}Sr/^{86}Sr$ of 0.70868 ± 0.00008; 1σ; n = 2), likely due to the low number of samples analyzed. Their corresponding $^{87}Sr/^{86}Sr$ are 0.708618 for sample KS032B, a mixture of oxalates and carbonated (hydroxyl)apatite (ideal composition $Ca_{10-x+u}\square_{x-u}(PO_4)_{6-x}(CO_3)_x(OH)_{2-x+2u}\square_{x-2u}$ where squares correspond to vacancies or additional cations and anions and $0<x<2$, $0<u<x$), and 0.708736 for the brushite KS006B sample (ideal composition [$CaHPO_4{\cdot}2(H_2O)$]).

Here, Sr ranges from 31.2 to 51.0 ppm in oxalates (median of 39.2 ppm), from 37.4 to 58.6 in phosphates (median of 48.0 ppm), and from 1.8 to 11.7 ppm in purines (median of 5.2 ppm) (Table S1). While in phosphates and oxalates Ca is a major element (22.5–25.0 wt%), in purine it mostly occurs as a trace element (<1 wt%) or more rarely as a minor component (5–6 wt%) (Table S1).

The isotope range for biominerals ($^{87}Sr/^{86}Sr$ from 0.707607 to 0.709970; Table 1) is largely within the one we obtained for a significant number of Italian drinking waters (0.706055–0.727360; Table 2 and Fig. 3). Water samples from the Pliocene-Quaternary volcanic aquifers of Mt. Vulture extinct volcano (Basilicata Region; samples BW8 and BW9) provide an $^{87}Sr/^{86}Sr$ of ~0.706055, the lowest ratio among the measured values. Conversely, waters from the Palaeozoic metamorphic aquifers of the Italian Alps, bottled in the towns of Forni Avoltri (near Udine, Friuli Venezia Giulia Region) and Valdidendro (near Sondrio, Lombardy Region) are characterized by the most radiogenic $^{87}Sr/^{86}Sr$: 0.717474 and 0.727360, for samples BW13 and BW17, respectively. The Palaeozoic intrusive complex of Sardinia Region (sample BW21) and Piedmont Region (sample BW28) provides a drinking water with a Sr ratio of 0.709712 and 0.712359, respectively (Table 2). Bottled waters coming from aquifers located in Mesozoic carbonate-rocks yield $^{87}Sr/^{86}Sr$ ranging from 0.707635 (sample BW5) to 0.708468 (sample BW6). Tap waters from Campania Region show a narrower range (Table 2 and Fig. 2), from 0.707659 for sample TW8 (Atripalda) to 0.707869 for sample TW5 (Bacoli), collected near Avellino and Napoli, respectively. More radiogenic values are observed for drinking waters from aquifers located in Cenozoic sedimentary calcareous and siliciclastic rocks (samples BW11, 12, 24 and 26) and in Quaternary glacial deposits (samples BW15 and 16) (Table 2). Intermediate isotope ratios are obtained for drinking waters from aquifers located in the Late-Pliocene calcareous hemipelagic sedimentary rocks (samples BW22 and BW23) of the Tuscany region (Table 2).

Sr concentrations in most of the drinking waters were gathered from the literature. For tap water, Sr ranged from 46.7 (TW1-2) to 639.8 ppb (TW4) with a median value of 269.4 ppb (Dinelli et al., 2012; Table S2). Bottled waters generally show a wider range of Sr concentrations, from 26 (BW14) to 2830.0 ppb (BW18), with a median value at ~677.7 ppb (Table S2). Calcium both for tap and bottled waters ranges from 12.5 to 313.0 ppm (Table S2).

In supplementary material are also reported different plots in order to verify possible correlation among Sr, Ca and $^{87}Sr/^{86}Sr$ ratios for both stone and water samples (Fig. S2). As a whole, Sr vs. Ca shows a strong linear correlation ($R^2 = 0.94$), mainly promoted by urinary stones, due to the ability of Sr^{2+} to substitute Ca^{2+} in the biomineral lattice. However, no correlation are observed between $^{87}Sr/^{86}Sr$ ratios vs. Ca or 1/Sr, generally suggesting that the strontium isotope fingerprint is influenced

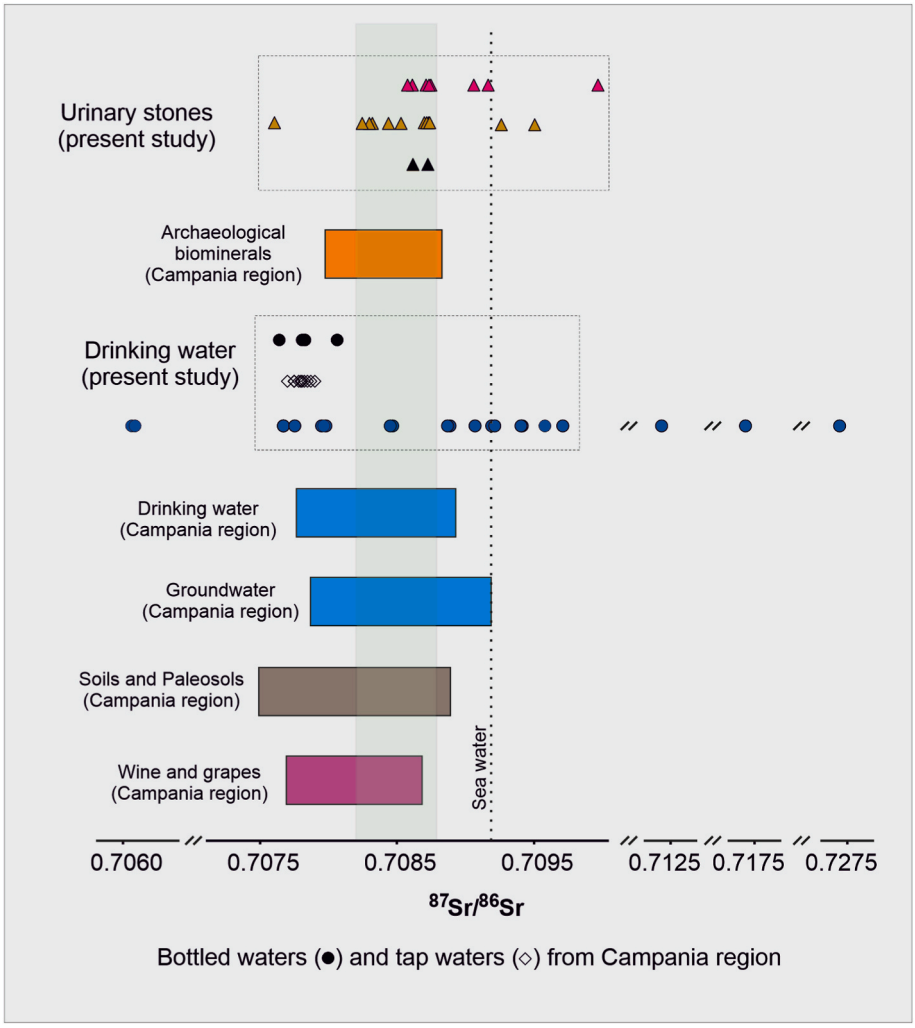

Figs. 4. $^{87}Sr/^{86}Sr$ ratios of studied biominerals and drinking waters. Data from the literature are also presented: archaeological biominerals (Arienzo et al., 2020; Tafuri et al., 2016); drinking water (Arienzo et al., 2020); groundwater (Arienzo et al., 2020; Sacchi et al., 2022); soils and paleosols (Arienzo et al., 2020; Emery et al., 2018; Tafuri et al., 2016); wine and grapes (Marchionni et al., 2013; Mercurio et al., 2014). The green field indicates the range of $^{87}Sr/^{86}Sr$ (0.70825–0.70874) of patients who declared drinking local waters and/or eat organic local foods. The local Naples seawater $^{87}Sr/^{86}Sr$ of 0.70919 was taken from (Arienzo et al., 2020). (For interpretation of the references to colour in this figure legend, the reader is referred to the Web version of this article.)

by the absolute concentration of Strontium or Calcium.

5. Discussion

In this study, the isotopic composition of strontium of uroliths from patients living in Campania Region was determined with the aim to assess the relationships between the $^{87}Sr/^{86}Sr$ values and the environment.

Sr could play a fundamental role in urolithiasis since it promotes (along with other trace elements such as cadmium, aluminum, copper, zinc, nickel and lead) the formation of poorly soluble salts (Bazin et al., 2007; Singh and Rai, 2014). Although Sr seems to differently concentrate in the diverse biominerals constituting uroliths, the corresponding $^{87}Sr/^{86}Sr$ ratios of calculi are totally independent from their mineralogical association. In fact, the Sr-isotope ratio of the oxalates, phosphates and purines roughly overlap (Fig. 3), centered at 0.70873 and ranging from 0.707607 (uricite KS020B) to 0.709970 (weddellite KS036B). These values clearly differs from the $^{87}Sr/^{86}Sr$ ratios available in the literature. Chinese patients from Beijing, for example, yielded higher values, from 0.70966 to 0.71099 (Qu et al., 2023).

As a whole, Sr isotope ratios in these studied biominerals and drinking waters are encopassed in the ranges reported for environmental matrices from Western Europe and Italy (Bataille et al., 2018; Lugli et al., 2022) (Fig. S1). However, due to the high variability of geological contexts, we elected to only consider the data available for the Campania Region and southern Italy (Lugli et al., 2022 and references therein). This allows a more reliable comparison between our uroliths and water samples.

When compared to other human biominerals, such as bones and teeth, collected from an archaeological site in Campania Region and other southeastern Italian sites (Arienzo et al., 2020; Tafuri et al., 2016), ranging from 0.70801 to 0.70880, our biomineral samples have a larger isotope range, which hints at, at least, one additional source of strontium, that may be external (Fig. 4). Archaeological biominerals from south Italy also show different ratios compared to those (mainly teeth) reported in literature for China areas (Li et al., 2013; Wang et al., 2020; Zhang et al., 2018), generally ranging from 0.70869 to 0.71161. Still, it can be noticed that Italian and Chinese biominerals (the only two available dataset for uroliths), can be discriminated by their $^{87}Sr/^{86}Sr$ ratios, likely as a consequence of the different environmental geological settings characterizing the two geographic areas.

As discussed, when comparing the Sr isotope ratios of our urinary stone samples with those previously published for archaeological biominerals (i.e., bones and teeth) from the exact same region, one can

observe a slight difference in the respective $^{87}Sr/^{86}Sr$ value ranges (urinary stones tend to yield more radiogenic values; Fig. 4). This evidence leads us to hypothesize external Sr inputs from the environmental matrices surrounding the patients and/or food/water from their daily dietary intake. The strontium isotope ratios of drinking waters have been shown to be a reliable hydro-geochemical tracer, mainly controlled by the mineralogical composition of the considered aquifer lithologies and their chronostratigraphic features (Bataille et al., 2018; Kim et al., 2013; Lugli et al., 2022; Ribeiro et al., 2014; Voerkelius et al., 2010). Generally, the lowest $^{87}Sr/^{86}Sr$ ratios (0.703–0.708) are encountered in groundwater circulating within younger volcanic formations such as, for example, Quaternary basalts. Conversely, older silicic (either igneous or metamorphic, crystalline) rocks generally display more radiogenic Sr isotope ratios, usually >0.709, as they contain high levels of Rb that produced high amounts of radiogenic ^{87}Sr through time. Intermediate $^{87}Sr/^{86}Sr$ values are expected for waters in aquifers interacting with limestone and calcareous/siliciclastic sediments (Ribeiro et al., 2014), mostly matching the Sr isotope composition of Meso-Cenozoic seawater (McArthur et al., 2020).

This trend is also valid for the drinking waters we analyzed. The less radiogenic bottled waters are from the Pliocene-Quaternary volcanic aquifers of Mt. Vulture ($^{87}Sr/^{86}Sr$ ratio around 0.70656), consistent with the Sr isotope ratios of volcanic products in this area (De Astis et al., 2006; Lugli et al., 2022 and references therein), and similar to natural mineral water samples from other European Tertiary and Quaternary volcanic rocks (Voerkelius et al., 2010). Similar values were also observed by Kim et al. (2013) for bottled waters related to Korean volcanic lithotypes, as well as for drinking waters bottled in Portugal from alkaline igneous rocks forming the *Monchique* aquifer (Ribeiro et al., 2014). On the other hand, our most radiogenic Sr isotope ratios are for bottled waters from the Palaeozoic metamorphic aquifers of the Italian Alps (0.717474 and 0.727436), and the Upper Carboniferous – Permian intrusive complex of Sardinia and Piedmont Regions (0.709712 and 0.712356). These values are similar to those of analogue contexts such as, for example, the aquifers in the Lower Palaeozoic and crystalline rocks of the old Variscan and Caledonian orogens (Voerkelius et al., 2010). Overall, the Sr isotope ratio of drinking waters, both bottled and from tap, broadly reflects the main aquifer-forming lithologies and, thus, the corresponding geological background. As aforementioned, aquifers in sedimentary rocks generally imprint intermediate radiogenic Sr ratios to groundwaters, usually between 0.706 and 0.710 (Ribeiro et al., 2014; Voerkelius et al., 2010). Here, the lowest ratios we measured are for waters bottled from aquifers in Mesozoic carbonate-rocks (i.e., marine limestones), whereas the remaining lithologies yield the highest ones (Table 2). Fig. 4 also shows that tap water samples, pumped from the same aquifer type, display $^{87}Sr/^{86}Sr$ ratios very similar to those of Campanian bottled waters as well as to regional soils, paleosols, wines and grapes (Arienzo et al., 2020, 2016; Lugli et al., 2022; Saar de Almeida et al., 2023; Sacchi et al., 2022). As expected, geological differences between the Campania Region and China reflect in the corresponding $^{87}Sr/^{86}Sr$ ratio of their soils and subsequently of their ground and drinking waters, with e.g., the southern Shaanxi Province having more radiogenic drinking waters (0.71050–0.71099) (Li et al., 2013). This range also includes that of the Miyun reservoir, the main surface source for drinking water in Beijing. As for our samples, the Sr isotope ratio overlap between kidney stones and drinking water is only partial for Beijing.

Italian drinking waters (both bottled and tap ones) mainly correspond to Mesozoic carbonate lithologies especially in the central and southern regions (De Vita et al., 2018; Fiorillo et al., 2019; Leone et al., 2023; Tufano et al., 2021). These rocks are formed by carbonate minerals such as calcite (ideal composition [$CaCO_3$]) and subordinately dolomite (ideal composition [$CaMg(CO_3)_2$]) that are particularly soluble. Thanks to this simple mineralogical composition, the Sr-isotope ratio of groundwaters in carbonate aquifers usually resemble that of their hosting rocks. This can be extended to aquifers located in evaporites. Other lithologies (i.e., non-carbonate aquifers) tend to have more variable Sr isotope ratios, that are defined by both varying dissolution rates and the exchange behaviors of the hosting rock minerals (e.g., feldspars, apatite, titanite, etc.) (Ribeiro et al., 2014). For example, the $^{87}Sr/^{86}Sr$ ratios of groundwaters from igneous, metamorphic and siliciclastic aquifers usually reflect those of their weathered minerals and rarely reach the more radiogenic Sr isotope ratio of the bulk rock.

Here, the overall range of drinking waters' $^{87}Sr/^{86}Sr$ overlaps that of the urinary stones (Fig. 4). As discussed, this can be first attributed to the water-rock interaction occurring in aquifers. The resulting Sr-isotope ratio is then transferred and preserved, through the food chain, to humans and animals and registered in their tissues, including pathological biominerals, without any isotope fractionation involving ^{87}Sr (Arienzo et al., 2020; Ribeiro et al., 2014; Voerkelius et al., 2010). This assumption is also supported by the overlap with the $^{87}Sr/^{86}Sr$ ratios of environmental matrices from the Campania Region, such as soils, paleosols, fossils (from shallow-water limestones of the Apennine Carbonate Platform of southern Italy), wines and grapes (Fig. 4). The $^{87}Sr/^{86}Sr$ ratios of all these matrices are generally lower than the ratio of 0.70919 determined for seawater in the gulf of Naples (Arienzo et al., 2020).

Still, the $^{87}Sr/^{86}Sr$ range of our urinary stones only partially matches that of the local environmental matrices, although it is in good agreement with that of Italian drinking waters (Fig. 4). This partial discrepancy may be explained by uncontrolled factors that may affect the conservativeness of the radiogenic Sr isotope ratio in pathological biominerals. For example, by mixing isotopically distinct Sr from either non-regional food and water sources or the natural or anthropogenic contamination of regional environmental matrices (i.e., soil and air) by: air pollution, fertilizers, aeolian dust coming from distal sources, etc. The range of $^{87}Sr/^{86}Sr$ reported for fertilizers is from 0.70335 to 0.71522 (Vitòria et al., 2004), and from 0.70920 to 0.71450 for animal manure and sewage (Widory et al., 2004b). Aerosols that are inhaled by the patients, on the other hand, have usually $^{87}Sr/^{86}Sr$ ratios >0.708, ranging from 0.70880 to 0.71532 (for $PM_{0.45}$ to PM_{10}) (Jung et al., 2019 and references therein), whereas typical urban emissions sources generate atmospheric particles with Sr isotope ratios between 0.708265 and 0.734413 (Widory et al., 2004a). Sr inputs by different means from these sources may thus explain the larger $^{87}Sr/^{86}Sr$ range we observe for urinary stones. In fact, it was already demonstrated that chronic kidney diseases are strictly associated with the exposure to particulate matter (i.e., $PM_{2.5}$ but also NO_2) occurring in polluted air of urbanized areas (Chu et al., 2023; Liang et al., 2021). Furthermore, considering the very low Sr concentration in drinking waters (from ~0.03 to ~2.8 ppm), other external Sr inputs may impact more significantly the $^{87}Sr/^{86}Sr$ ratios of urinary stones. For example, animal manures have Sr contents varying between 3.2 and 38.3 ppm (Widory et al., 2004b), whereas in wine ranges are from 0.05 up to 2827 ppb (Angus et al., 2006; Coldwell et al., 2022; Lancellotti et al., 2021; Mercurio et al., 2014). Again, the Sr contents of milk and dairy products can be as high as 6.35 ppm (Almášiová et al., 2023; Filippini et al., 2020). Lastly, the potential effect of the patients' geographical mobility, as well as the duration of the biomineral growth have to be considered too. In our study, all patients lived all their life in the Campania Region. It is noteworthy that although most of them stated during their clinical interviews that they have been drinking local wines every day (Mercurio et al., 2022), only 36% of them declared eating local organic food and/or drinking local waters. For this particular group (identified by a green field in Fig. 4), their corresponding biominerals delimited a narrower $^{87}Sr/^{86}Sr$ range roughly matching those of regional geological materials and waters, as well as those of archaeological biominerals.

6. Conclusions

Urolithiasis is a rather common pathology among the adult population and the biominerals it produces, i.e., urinary stones, may represent

a potential proxy to characterize the environmental matrices that surrounded patients before being diagnosed. Actually, the presence of Sr in human urine contributes to the formation of poorly soluble salts, and consequently the growth of urinary stones. Coupling the morpho-constitutional classification of biominerals and their $^{87}Sr/^{86}Sr$ ratios, and comparing them with the Sr-isotope characteristics of potential regional sources of strontium, we tried to better understand the possible relations among these different Sr reservoirs. This led to the following conclusions:

- The 21 urinary stones were classified as calcium oxalates, purines, and calcium phosphates. The difference in their mineralogy appears to be only partly reflected in their $^{87}Sr/^{86}Sr$ with the oxalates having slightly more radiogenic isotope ratios than purines, and calcium phosphates yielding a narrower intermediate isotope range (that may only result from the low number of samples analyzed).
- Globally, the $^{87}Sr/^{86}Sr$ range measured in our biominerals overlaps that of Italian drinking waters (tap and bottled waters). But on a smaller geographic area, i.e., the Campania region, our results show that $^{87}Sr/^{86}Sr$ ratios in biominerals are slightly different from those characterizing regional waters, soils, food… This hints at the fact that additional sources of strontium should be considered, such as for example agriculture practices, reflected in some types of food and beverages, or inhaled aerosols. These have typical $^{87}Sr/^{86}Sr$ ratios that may help explain this isotope difference.

This preliminary study evidences how the strontium isotope ratio of urinary stones records that of the patient's surroundings environmental matrices, although further investigations will be necessary to confirm this hypothesis. In particular, expanding the collection and analysis of pathological biominerals is required as well as including samples from various areas of Italy, characterized by distinct geological settings (Apennine, Alpine, Quaternary volcanic areas…). This should allow reinforcing the expected isotope linking between the geological substrate and the geochemical parameters of urinary stones. This will ultimately establish pathological biominerals as a new family of reliable biomonitoring proxies. They can then be integrated in creating Sr-isotope isoscapes that may serve in public health, occupational medicine, forensic investigations, migration or human provenance studies.

Credit author statement

David Widory: Writing – review & editing, Writing – original draft, Conceptualization. Luigi Salzano: Writing – review & editing, Resources. Chiara Germinario: Writing – review & editing, Formal analysis. Celestino Grifa: Writing – review & editing, Formal analysis. Ettore Varricchio: Writing – review & editing. Mariano Mercurio: Writing – review & editing, Writing – original draft, Supervision, Project administration, Methodology, Funding acquisition, Conceptualization. Francesco Izzo: Writing – review & editing, Writing – original draft, Visualization, Methodology, Investigation, Formal analysis, Data curation, Conceptualization. Valeria Di Renzo: Writing – original draft, Visualization, Methodology, Investigation, Formal analysis, Data curation, Conceptualization. Alessio Langella: Writing – review & editing, Writing – original draft, Supervision, Project administration, Methodology, Funding acquisition, Conceptualization. Massimo D'Antonio: Writing – review & editing, Writing – original draft, Supervision, Resources, Methodology, Conceptualization. Piergiorgio Tranfa: Writing – review & editing, Visualization, Investigation, Formal analysis.

Declaration of competing interest

The authors declare that they have no known competing financial interests or personal relationships that could have appeared to influence the work reported in this paper.

Data availability

All data are reported in the manuscript and in references therein.

Acknowledgements

The authors would like to thank the Editor Hefa Cheng and two anonymous referees for their valuable and significant suggestions, which greatly improved the manuscript. The authors also thank: Armando Orlacchio for his collaboration during bibliographic research; Dr. Vincenzo Monetti and Lisa Maria Francese for their costant and valuable assistance for ICP-OES analyses (and so much more); Prof. Domenico Cicchella for kindly provide data on Sr and Ca concentrations in drinking waters; Dr. Giuseppe Lotrecchiano, Dr. Pietro Saldutto and Dr. Maria Chiara Di Meo for their collaboration in the first steps of the present investigation. FRA 2020 "Caratterizzazione mineralogica di calcoli urinari mediante approccio multimetodologico" (University of Sannio, Department of Science and Technology), granted to Mariano Mercurio and Alessio langella, funded this study.

Appendix A. Supplementary data

Supplementary data to this article can be found online at https://doi.org/10.1016/j.envpol.2024.123316.

References

Abdel-Gawad, M., Ali-El-Dein, B., Elsobky, E., Mehta, S., Alsaigh, N., Knoll, T., Kura, M., Kamphuis, G., Alhayek, S., Alkohlany, K., Buchholz, N., Monga, M., 2022. Micro-elemental analysis and characterization of major heavy metals and trace elements in the urinary stones collected from patients living in diverse geographical regions. Environ. Sci. Pollut. Res. 29, 68941–68949. https://doi.org/10.1007/s11356-022-20732-x.

Almášiová, S., Toman, R., Pšenková, M., Tančin, V., Mikláš, Š., Jančo, I., 2023. Chemical elements content in goat milk, whey, cheese and yogurt from an ecological and conventional farm in Slovakia. J. Cent. Eur. Agric. 24, 43–52.

Angus, N.S., O'Keeffe, T.J., Stuart, K.R., Miskelly, G.M., 2006. Regional classification of New Zealand red wines using inductively-coupled plasma-mass spectrometry (ICP-MS). Aust. J. Grape Wine Res. 12, 170–176. https://doi.org/10.1111/j.1755-0238.2006.tb00057.x.

Arienzo, I., Fedele, A., Capuozzo, B., Tamburrino, S., Liotta, M., Somma, R., 2016. Sr isotope analysis of water samples at the radiogenic isotope laboratory of the Istituto Nazionale Di Geofisica E Vulcanologia, sezione di Napoli-Osservatorio Vesuviano (INGV-OV). Rapp. Tec. INGV. https://doi.org/10.13140/RG.2.1.4377.1285.

Arienzo, I., Rucco, I., Di Vito, M.A., D'Antonio, M., Cesarano, M., Carandente, A., De Angelis, F., Romboni, M., Rickards, O., 2020. Sr isotopic composition as a tool for unraveling human mobility in the Campania area. Archaeol. Anthropol. Sci. 12, 157. https://doi.org/10.1007/s12520-020-01088-0.

Athanasiadou, D., 2017. New insights into the chemical and isotopic composition of human-body biominerals. II: COM kidney stones from Greece. Int. Arch. Urol. Complicat. 3 (3) https://doi.org/10.23937/2469-5742/1510020, 020.

Athanasiadou, D., Godelitsas, A., Sokaras, D., Karydas, A.G., Dotsika, E., Potamitis, C., Zervou, M., Xanthos, S., Chatzitheodoridis, E., Gooi, H.C., Becker, U., 2013. New insights into the chemical and isotopic composition of human-body biominerals. I: cholesterol gallstones from England and Greece. J. Trace Elem. Med. Biol. 27, 79–84. https://doi.org/10.1016/j.jtemb.2012.08.004.

Basavaraj, D.R., Biyani, C.S., Browning, A.J., Cartledge, J.J., 2007. The role of urinary kidney stone inhibitors and promoters in the pathogenesis of calcium containing renal stones{A figure is presented. EAU-EBU Update Ser. 5, 126–136. https://doi.org/10.1016/j.eeus.2007.03.002.

Bataille, C.P., von Holstein, I.C.C., Laffoon, J.E., Willmes, M., Liu, X.-M., Davies, G.R., 2018. A bioavailable strontium isoscape for Western Europe: a machine learning approach. PLoS One 13, e0197386.

Bazin, D., Chevallier, P., Matzen, G., Jungers, P., Daudon, M., 2007. Heavy elements in urinary stones. Urol. Res. 35, 179–184. https://doi.org/10.1007/s00240-007-0099-z.

Capo, R.C., Stewart, B.W., Chadwick, O.A., 1998. Strontium isotopes as tracers of ecosystem processes: theory and methods. Geoderma 82, 197–225. https://doi.org/10.1016/S0016-7061(97)00102-X.

Chandrajith, R., Weerasingha, A., Premaratne, K.M., Gamage, D., Abeygunasekera, A.M., Joachimski, M.M., Senaratne, A., 2019. Mineralogical, compositional and isotope characterization of human kidney stones (urolithiasis) in a Sri Lankan population. Environ. Geochem. Health 41, 1881–1894. https://doi.org/10.1007/s10653-018-0237-2.

Chu, L., Chen, K., Di, Q., Crowley, S., Dubrow, R., 2023. Associations between short-term exposure to PM2.5, NO2 and O3 pollution and kidney-related conditions and the role of temperature-adjustment specification: a case-crossover study in New York state. Environ. Pollut. 328, 121629 https://doi.org/10.1016/j.envpol.2023.121629.

Cicchella, D., Albanese, S., De Vivo, B., Dinelli, E., Giaccio, L., Lima, A., Valera, P., 2010. Trace elements and ions in Italian bottled mineral waters: identification of anomalous values and human health related effects. J. Geochem. Explor. 107, 336–349. https://doi.org/10.1016/j.gexplo.2010.04.004.

Cloutier, J., Villa, L., Traxer, O., Daudon, M., 2015. Kidney stone analysis: "Give me your stone, I will tell you who you are!". World J. Urol. 33, 157–169. https://doi.org/10.1007/s00345-014-1444-9.

Coelho, I., Castanheira, I., Bordado, J.M., Donard, O., Silva, J.A.L., 2017. Recent developments and trends in the application of strontium and its isotopes in biological related fields. TrAC - Trends Anal. Chem. 90, 45–61. https://doi.org/10.1016/j.trac.2017.02.005.

Coldwell, B.C., Pérez, N.M., Vaca, M.C., Pankhurst, M.J., Hernández, P.A., Rodriguez, G. V.M., Padrón, E., Asensio-Ramos, M., Ribeiro, S., Santos, J.F., 2022. Strontium isotope systematics of tenerife wines (canary Islands): tracing provenance in ocean Island terroir. Beverages. https://doi.org/10.3390/beverages8010009.

Crowley, B.E., Miller, J.H., Bataille, C.P., 2017. Strontium isotopes (87Sr/86Sr) in terrestrial ecological and palaeoecological research: empirical efforts and recent advances in continental-scale models. Biol. Rev. 92, 43–59. https://doi.org/10.1111/brv.12217.

D'Antonio, M., Di Renzo, V., Arienzo, I., Widory, D., 2023. Isotopic analysis techniques applied to forensics: new frontiers of isotope geochemistry BT - mineralogical analysis applied to forensics: a guidance on mineralogical techniques and their application to the forensic field. In: Mercurio, M., Langella, A., Di Maggio, R.M., Cappelletti, P. (Eds.), Mineralogical Analysis Applied to Forensics A Guidance on Mineralogical Techniques and Their Application to the Forensic Field. Springer International Publishing, Cham, pp. 251–290. https://doi.org/10.1007/978-3-031-08834-6_9.

Daudon, M., Dessombz, A., Frochot, V., Letavernier, E., Haymann, J.P., Jungers, P., Bazin, D., 2016. Comprehensive morpho-constitutional analysis of urinary stones improves etiological diagnosis and therapeutic strategy of nephrolithiasis. Compt. Rendus Chem. 19, 1470–1491. https://doi.org/10.1016/j.crci.2016.05.008.

De Astis, G., Kempton, P.D., Peccerillo, A., Wu, T.W., 2006. Trace element and isotopic variations from Mt. Vulture to Campanian volcanoes: constraints for slab detachment and mantle inflow beneath southern Italy. Contrib. Mineral. Petrol. 151, 331–351. https://doi.org/10.1007/s00410-006-0062-y.

De Vita, P., Allocca, V., Celico, F., Fabbrocino, S., Mattia, C., Monacelli, G., Musilli, I., Piscopo, V., Scalise, A.R., Summa, G., 2018. Hydrogeology of continental southern Italy. J. Maps 14, 230–241. https://doi.org/10.1080/17445647.2018.1454352.

Diangienda, P.K.D., Moningo, D.M., Mayindu, A.N., Haymann, J.-P., Daudon, M., 2021. Heavy metals in urinary stones in the Democratic Republic of Congo. Afr. J. Urol. 27, 1–9. https://doi.org/10.1186/s12301-021-00188-0.

Dinelli, E., Lima, A., Albanese, S., Birke, M., Cicchella, D., Giaccio, L., Valera, P., De Vivo, B., 2012. Major and trace elements in tap water from Italy. J. Geochem. Explor. 112, 54–75. https://doi.org/10.1016/j.gexplo.2011.07.009.

Emery, M.V., Stark, R.J., Murchie, T.J., Elford, S., Schwarcz, H.P., Prowse, T.L., 2018. Mapping the origins of Imperial Roman workers (1st–4th century CE) at Vagnari, Southern Italy, using 87Sr/86Sr and δ18O variability. Am. J. Phys. Anthropol. 166, 837–850. https://doi.org/10.1002/ajpa.23473.

Faure, G., Mensing, T.M., 2004. Isotopes: Principles and Applications, third ed. Wiley.

Filippini, T., Tancredi, S., Malagoli, C., Malavolti, M., Bargellini, A., Vescovi, L., Nicolini, F., Vinceti, M., 2020. Dietary estimated intake of trace elements: risk assessment in an Italian population. Expo. Heal. 12, 641–655. https://doi.org/10.1007/s12403-019-00324-w.

Fiorillo, F., Leone, G., Pagnozzi, M., Catani, V., Testa, G., Esposito, L., 2019. The Upwelling Groundwater Flow in the Karst Area of Grassano-Telese Springs (Southern Italy). Water. https://doi.org/10.3390/w11050872.

Font, L., van der Peijl, G., van Wetten, I., Vroon, P., van der Wagt, B., Davies, G., 2012. Strontium and lead isotope ratios in human hair: investigating a potential tool for determining recent human geographical movements. J. Anal. At. Spectrom. 27, 719–732. https://doi.org/10.1039/C2JA10361C.

Frassetto, L., Kohlstadt, I., 2011. Treatment and prevention of kidney stones: an Update. Am. Fam. Physician 84, 1234–1242.

Frei, K.M., Price, T.D., 2012. Strontium isotopes and human mobility in prehistoric Denmark. Archaeol. Anthropol. Sci. 4, 103–114. https://doi.org/10.1007/s12520-011-0087-7.

Giannossi, M.L., Summa, V., Mongelli, G., 2013. Trace element investigations in urinary stones: a preliminary pilot case in Basilicata (Southern Italy). J. Trace Elem. Med. Biol. 27, 91–97. https://doi.org/10.1016/j.jtemb.2012.09.004.

Goldstein, S.L., Oelkers, E.H., Rudnick, R.L., Walter, L.M., 2003. Standards for publication of isotope ratio and chemical data in Chemical Geology. Chem. Geol. 202, 1–4. https://doi.org/10.1016/j.chemgeo.2003.08.003.

Holt, E., Evans, J.A., Madgwick, R., 2021. Strontium (87Sr/86Sr) mapping: a critical review of methods and approaches. Earth Sci. Rev. 216, 103593 https://doi.org/10.1016/j.earscirev.2021.103593.

Huang, J., Luo, L., Wang, Yongbo, Yan, S., Li, X., Li, B., Huang, Q., Wang, Yunyun, Zhang, Y., Wei, S., Wang, Yibaina, Zeng, X., 2023. The burden of chronic kidney disease associated with dietary exposure to cadmium in China, 2020. Environ. Pollut. 336, 122434 https://doi.org/10.1016/j.envpol.2023.122434.

Izzo, F., Langella, A., Germinario, C., Grifa, C., Varricchio, E., Di Meo, M.C., Salzano, L., Lotrecchiano, G., Mercurio, M., 2022. Morpho-constitutional classification of urinary stones as prospective approach for the management of human pathological biomineralization: new insights from southern Italy. Minerals. https://doi.org/10.3390/min12111421.

Jain, R.B., 2020. Cadmium and kidney function: concentrations, variabilities, and associations across various stages of glomerular function. Environ. Pollut. 256, 113361 https://doi.org/10.1016/j.envpol.2019.113361.

James, H.F., Adams, S., Willmes, M., Mathison, K., Ulrichsen, A., Wood, R., Valera, A.C., Frieman, C.J., Grün, R., 2022. A large-scale environmental strontium isotope baseline map of Portugal for archaeological and paleoecological provenance studies. J. Archaeol. Sci. 142, 105595 https://doi.org/10.1016/j.jas.2022.105595.

Jung, C.-C., Chou, C.C.-K., Lin, C.-Y., Shen, C.-C., Lin, Y.-C., Huang, Y.-T., Tsai, C.-Y., Yao, P.-H., Huang, C.-R., Huang, W.-R., Chen, M.-J., Huang, S.-H., Chang, S.-C., 2019. C-Sr-Pb isotopic characteristics of PM2.5 transported on the East-Asian continental outflows. Atmos. Res. 223, 88–97. https://doi.org/10.1016/j.atmosres.2019.03.011.

Kenoyer, J.M., Price, T.D., Burton, J.H., 2013. A new approach to tracking connections between the Indus Valley and Mesopotamia: initial results of strontium isotope analyses from Harappa and Ur. J. Archaeol. Sci. 40, 2286–2297. https://doi.org/10.1016/j.jas.2012.12.040.

Kim, G.-E., Shin, W.-J., Ryu, J.-S., Choi, M.-S., Lee, K.-S., 2013. Identification of the origin and water type of various Korean bottled waters using strontium isotopes. J. Geochem. Explor. 132, 1–5. https://doi.org/10.1016/j.gexplo.2013.03.002.

Kuta, J., Machát, J., Benová, D., Červenka, R., Kořistková, T., 2012. Urinary calculi - atypical source of information on mercury in human biomonitoring. Cent. Eur. J. Chem. 10, 1475–1483. https://doi.org/10.2478/s11532-012-0063-9.

Kuta, J., Machát, J., Benová, D., Červenka, R., Zeman, J., Martinec, P., 2013. Association of minor and trace elements with mineralogical constituents of urinary stones: a hard nut to crack in existing studies of urolithiasis. Environ. Geochem. Health 35, 511–522.

Lancellotti, L., Sighinolfi, S., Ulrici, A., Maletti, L., Durante, C., Marchetti, A., Tassi, L., 2021. Tracing geographical origin of Lambrusco PDO wines using isotope ratios of oxygen, boron, strontium, lead and their elemental concentration. Curr. Res. Food Sci. 4, 807–814. https://doi.org/10.1016/j.crfs.2021.11.001.

Leone, G., D'Agostino, N., Esposito, L., Fiorillo, F., 2023. Hydrological deformation of karst aquifers detected by GPS measurements, Matese massif, Italy. Environ. Earth Sci. 82, 240. https://doi.org/10.1007/s12665-023-10905-3.

Li, Z., He, M., Peng, B., Jin, Z., 2013. Strontium concentrations and isotope ratios in enamel of healthy and carious teeth in southern Shaanxi, China. Rapid Commun. Mass Spectrom. 27, 1919–1924. https://doi.org/10.1002/rcm.6646.

Liang, Z., Wang, W., Wang, Y., Ma, L., Liang, C., Li, P., Yang, C., Wei, F., Li, S., Zhang, L., 2021. Urbanization, ambient air pollution, and prevalence of chronic kidney disease: a nationwide cross-sectional study. Environ. Int. 156, 106752 https://doi.org/10.1016/j.envint.2021.106752.

Lugli, F., Cipriani, A., Bruno, L., Ronchetti, F., Cavazzuti, C., Benazzi, S., 2022. A strontium isoscape of Italy for provenance studies. Chem. Geol. 587, 120624 https://doi.org/10.1016/j.chemgeo.2021.120624.

Marchionni, S., Braschi, E., Tommasini, S., Bollati, A., Cifelli, F., Mulinacci, N., Mattei, M., Conticelli, S., 2013. High-precision 87Sr/86Sr analyses in wines and their use as a geological fingerprint for tracing geographic provenance. J. Agric. Food Chem. 61, 6822–6831. https://doi.org/10.1021/jf4012592.

McArthur, J.M., Howarth, R.J., Shields, G.A., Zhou, Y., 2020. Chapter 7 - strontium isotope stratigraphy. In: Gradstein, F.M., Ogg, J.G., Schmitz, M.D., Ogg (Eds.), Geologic Time Scale 2020. Elsevier, pp. 211–238. https://doi.org/10.1016/B978-0-12-824360-2.00007-3. G.M.B.T.-G.T.S. 2020.

Mercurio, M., Grilli, E., Odierna, P., Morra, V., Prohaska, T., Coppola, E., Grifa, C., Buondonno, A., Langella, A., 2014. A "Geo-Pedo-Fingerprint" (GPF) as a tracer to detect univocal parent material-to-wine production chain in high quality vineyard districts, Campi Flegrei (Southern Italy). Geoderma 231, 64–78. https://doi.org/10.1016/j.geoderma.2014.04.006, 230.

Mercurio, M., Izzo, F., Gatta, G.D., Salzano, L., Lotrecchiano, G., Saldutto, P., Germinario, C., Grifa, C., Varricchio, E., Carafa, A., 2022. A comprehensive mineralogical study of a jackstone calculus and some other human bladder stones unveil health and environmental implications? Environ. Geochem. Health 44, 3297–3320. https://doi.org/10.1007/s10653-021-01083-x.

Ministry of Health, I., 2016. Conoscere l'acqua del proprio rubinetto [WWW Document]. Conosc. l'acqua del proprio rubinetto. URL. https://www.salute.gov.it/portale/temi/p2_6.jsp?lingua=italiano&id=4528&area=acque_potabili&menu=dieta.

Pal'chik, N.A., Moroz, T.N., Maksimova, N.V., Dar'in, A.V., 2006. Mineral and microelement compositions of urinary stones. Russ. J. Inorg. Chem. 51, 1098–1105. https://doi.org/10.1134/S0036023606070138.

Price, T.D., Burton, J.H., Fullagar, P.D., Wright, L.E., Buikstra, J.E., Tiesler, V., 2008. Strontium isotopes and the study of human mobility in ancient mesoamerica. Lat. Am. Antiq. 19, 167–180. https://doi.org/10.1017/S1045663500007781.

Price, T.D., Gestsdóttir, H., 2006. The first settlers of Iceland: an isotopic approach to colonisation. Antiquity 80, 130–144. https://doi.org/10.1017/S0003598X00093315.

Qu, R., Han, G., Tian, Y., Zhao, Y., 2023. Strontium isotope ratios in kidney stones reveal the environmental implications for humans in Beijing, China. Environ. Geochem. Health. https://doi.org/10.1007/s10653-023-01515-w.

Ribeiro, S., Azevedo, M.R., Santos, J.F., Medina, J., Costa, A., 2014. Sr isotopic signatures of Portuguese bottled mineral waters and their relationships with the geological setting. Comun. Geológicas 101, 29–37.

Saar de Almeida, B., Fedele, L., D'Antonio, M., Morra, V., Mercurio, M., Stevenson, R., Widory, D., 2023. Characterizing wine terroir using strontium isotope ratios: a review. Isot. Environ. Health Stud. 1–22. https://doi.org/10.1080/10256016.2023.2245122.

Sacchi, E., Cuoco, E., Oster, H., Paolucci, V., Tedesco, D., Viaroli, S., 2022. Tracing groundwater circulation in a valuable mineral water basin with geochemical and isotopic tools: the case of FERRARELLE, Riardo basin. Southern Italy. Environ. Geochem. Health 44, 1–28. https://doi.org/10.1007/s10653-021-00845-x.

Singh, V.K., Rai, P.K., 2014. Kidney stone analysis techniques and the role of major and trace elements on their pathogenesis: a review. Biophys. Rev. 6, 291–310. https://doi.org/10.1007/s12551-014-0144-4.

Sorokin, I., Mamoulakis, C., Miyazawa, K., Rodgers, A., Talati, J., Lotan, Y., 2017. Epidemiology of stone disease across the world. World J. Urol. 35, 1301–1320. https://doi.org/10.1007/s00345-017-2008-6.

Stantis, C., Kinaston, R.L., Richards, M.P., Davidson, J.M., Buckley, H.R., 2015. Assessing human diet and movement in the Tongan maritime chiefdom using isotopic analyses. PLoS One 10, e0123156.

Stewart, B.W., Capo, R.C., Chadwick, O.A., 1998. Quantitative strontium isotope models for weathering, pedogenesis and biogeochemical cycling. Geoderma 82, 173–195. https://doi.org/10.1016/S0016-7061(97)00101-8.

Sun, Y., Zhou, Q., Zheng, J., 2019. Nephrotoxic metals of cadmium, lead, mercury and arsenic and the odds of kidney stones in adults: an exposure-response analysis of NHANES 2007–2016. Environ. Int. 132, 105115 https://doi.org/10.1016/j.envint.2019.105115.

Tafuri, M.A., Fullagar, P.D., O'Connell, T.C., Belcastro, M.G., Iacumin, P., Conati Barbaro, C., Sanseverino, R., Robb, J., 2016. Life and death in neolithic southeastern Italy: the strontium isotopic evidence. Int. J. Osteoarchaeol. 26, 1045–1057. https://doi.org/10.1002/oa.2516.

Thomas, L.D.K., Elinder, C.-G., Tiselius, H.-G., Wolk, A., Åkesson, A., 2013. Dietary cadmium exposure and kidney stone incidence: a population-based prospective cohort study of men & women. Environ. Int. 59, 148–151. https://doi.org/10.1016/j.envint.2013.06.008.

Tian, Y., Han, G., Qu, R., Xiao, C., 2022. Major and trace elements in human kidney stones: a preliminary investigation in Beijing, China. Minerals 12, 512. https://doi.org/10.3390/min12050512.

Tufano, R., Formetta, G., Calcaterra, D., De Vita, P., 2021. Hydrological control of soil thickness spatial variability on the initiation of rainfall-induced shallow landslides using a three-dimensional model. Landslides 18, 3367–3380. https://doi.org/10.1007/s10346-021-01681-x.

van der Aa, M., 2003. Classification of mineral water types and comparison with drinking water standards. Environ. Geol. 44, 554–563. https://doi.org/10.1007/s00254-003-0791-4.

Vitòria, L., Otero, N., Soler, A., Canals, À., 2004. Fertilizer characterization: isotopic data (N, S, O, C, and Sr). Environ. Sci. Technol. 38, 3254–3262. https://doi.org/10.1021/es0348187.

Voerkelius, S., Lorenz, G.D., Rummel, S., Quétel, C.R., Heiss, G., Baxter, M., Brach-Papa, C., Deters-Itzelsberger, P., Hoelzl, S., Hoogewerff, J., Ponzevera, E., Van Bocxstaele, M., Ueckermann, H., 2010. Strontium isotopic signatures of natural mineral waters, the reference to a simple geological map and its potential for authentication of food. Food Chem. 118, 933–940. https://doi.org/10.1016/j.foodchem.2009.04.125.

Wang, L., Chen, M., He, P., Yu, H., Block, K.A., Xie, Z., 2019. Composition and spatial distribution of elements and isotopes of a giant human bladder stone and environmental implications. Sci. Total Environ. 650, 835–846.

Wang, X., Shen, H., Wei, D., Hu, X., Xu, B., Qin, X., Tang, Z., 2020. Human mobility in the lop Nur region during the Han-Jin Dynasties: a multi-approach study. Archaeol. Anthropol. Sci. 12, 20. https://doi.org/10.1007/s12520-019-00956-8.

Wang, X., Tang, Z., 2020. The first large-scale bioavailable Sr isotope map of China and its implication for provenance studies. Earth Sci. Rev. 210, 103353 https://doi.org/10.1016/j.earscirev.2020.103353.

WHO, W.H.O., 2010. Concise international chemical assessment document 77". Strontium and strontium compounds 978, 4.

Widory, D., Fiani, E., Le Moullec, Y., Gruson, Y., Gayrard, O., 2004a. Développement d'une méthode de caractérisation des contributions des sources fixes aux émissions atmosphériques de particules utilisant le traçage multi-isotopique. Appl. au cas l'Agglomération Parisienne 115.

Widory, D., Kloppmann, W., Chery, L., Bonnin, J., Rochdi, H., Guinamant, J.-L., 2004b. Nitrate in groundwater: an isotopic multi-tracer approach. J. Contam. Hydrol. 72, 165–188. https://doi.org/10.1016/j.jconhyd.2003.10.010.

Zhang, W., Hu, Z., 2020. Estimation of isotopic reference values for pure materials and geological reference materials. At. Spectrosc 41, 93–102. https://doi.org/10.46770/AS.2020.03.001.

Zhang, X.X., Wang, X.R., Wu, X.T., Jin, Z.Y., Zhang, H.R., Huang, F., 2018. Investigating human migration and Horse-Trading in Yelang (夜郎) through strontium isotope analysis of skeletons from Zhougshui sites, south-West China (1300 bc – ad 25). Archaeometry 60, 157–170. https://doi.org/10.1111/arcm.12365.